The impact of roof systems on cooling and building energy efficiency

Yihang Wang[a], Zhi-Hua Wang[a*], Negar Rahmatollahi[a], Haoran Hou[b]

[a] *School of Sustainable Engineering and the Built Environment, Arizona State University, Tempe, USA*

[b] *State Key Laboratory of Urban and Regional Ecology, Research Center for Eco-Environmental Sciences, Chinese Academy of Sciences, Beijing 100085, China*

[*] Corresponding author. Email: zhwang@asu.edu. Tel: +1-480-727-2933

Abstract

The excessive warming in the built environment, due to urbanization and anthropogenic heat emissions, has adverse effects on building energy consumption. Diverse technology using, e.g., vegetated roofs or innovative roof materials, have been proposed to ameliorate both indoor and outdoor thermal environments and reduce energy consumption. In this study, we apply a state-of-the-art urban canopy model to simulate the thermal performance of multiple roof technology, viz. the white, green, and hybrid roofs, in the contrasting urban environments of Princeton, NJ and Phoenix, AZ, USA. In addition, we estimate the combined energy-water saving potential for green roofs with five different irrigation schemes. It is found that green roofs can achieve a combined energy-water saving of \$9.68 m^{-2} roof area in Phoenix with moisture-controlled irrigation, and \$5.23 m^{-2} in Princeton without irrigation. These results can help to promote building energy efficiency by adapting to flexible and sustainable roof technology for heat mitigation.

Keywords: Albedo; Energy-water trade-off; Green roofs; Heat mitigation; Urban irrigation; Urban canopy model

1. Introduction

Urban areas accommodate 56% of world population, consume over two thirds of world's energy, and produce about 70% of global carbon emissions today [1][2]. The global urbanization has led to critical environmental challenges, including excessive heat stress, air pollution, infrastructure vulnerability, and degraded ecosystems [3][4][5], to name a few. Many of the adverse environmental effect of urbanization can be traced back to or strongly regulated by the exacerbated thermal environment in cities, a prominent example being the urban heat island (UHI) effect [6]. The change of urban thermal environment, especially ambient air temperature, has induced notable increase in building energy consumption [9][10], which accounts for 60% of the global primary energy requirement and generates about 33% of all the greenhouse gas (GHG) emissions [1]. Such a large amount of energy consumption, in turn, elevates the warming trend of the urban environment, imposing critical challenges for climate change mitigation and the development of sustainable cities [12].

While background climate conditions, e.g. radiative forcings or synoptic pressure systems, are critical in regulating the urban thermal environment [13], it is the landscape characteristics that can be actively managed by urban planners for sustainable urban development. Among many landscape contributors to the exacerbation of urban thermal environment, the lack of green spaces and changes of thermal properties of pavement materials, especially the reflectivity to solar radiation (i.e. albedo), are the primary attributes [14]. Among the built-up surfaces, roofs have comparable horizontal coverage, but relatively higher degree of freedom and lower deployment and maintenance cost for heat mitigation strategies, as compared to street canyon facets (walls, roads, and ground) [15]. Such advantage makes roof engineering a promising solution to ameliorate the livability of urban environment and, in particular, to cut back building energy consumption. The most commonly adopted roof engineering technology includes the use of white or super-white roofs (with high to ultra-high albedo) and green roofs (vegetated with irrigation). White roofs (also known as "cool" roofs) help to reduce the skin temperature of paved surfaces and the indoor energy consumption [16][18]. According to previous studies, by reflecting more shortwave radiation back to the atmosphere, white roofs are capable of lowering temperatures of roof surfaces, indoor ceilings, and ambient air significantly, hence reducing the indoor cooling demand for 5-50% [19]. Nevertheless, the cooling and energy saving potentials of white roofs are often accompanied by unintended consequences such as heating penalty, i.e. the increase of heating load in cold seasons due to lowered indoor temperatures, or other adverse effects [20].

One particular countermeasure to the heating penalty was proposed by reducing the roof albedo (black roofs) for buildings in the cool season, hence, enhancing the building energy efficiency [23]. More generally, engineering of temperature-adaptive roofs that are capable of adjusting its surface albedo according to the ambient temperature by using thermochromic materials, i.e. the hybrid roof, were proposed and tested, which is effective for providing cooling in summer and warming effect in winter [24]. In the past decades, several different hybrid roof structures have been designed and implemented, with most of them containing multiple layers that consist of metal and nonmetal compounds like VO_2, MgF_2, and BaF_2 that could change the albedo in a certain temperature interval, and metals like tungsten W and germanium Ge, which could modulate the transition temperature of thermal properties of the roof structures [26]. Related studies show that hybrid roofs can save up to 11% of the annual energy consumption of buildings in comparison to conventional roofs [29]. Though showing promising potentials on energy savings, challenges remain which limit the practical applications of hybrid roofs. To achieve the maximum energy savings, the transition temperatures of the roof structure need to be controlled within a small interval that vary with climates (generally from 20℃ to 28℃), while the transition temperatures of different thermochromic materials vary significantly (from −170°C to 100°C). This make the design of hybrid roofs challenging since the components need to be controlled accurately to achieve the desired transition temperatures. Besides, due to the complexity of the components and structures of temperature-adaptive roofs, the fabrication procedures are complicated and time-consuming, which also hinders their promotion in practical engineering [25].

The technology of white or hybrid roofs is based purely on the change of surface albedo of roof surfaces and aims to provide a "simple" solution to the excessive heat problem in urban areas, especially for UHI mitigation. Nevertheless, it is becoming increasingly clear that UHI is not a stand-alone problem but instead closely interwoven with other anthropogenically induced environmental issues, such as the concentrated emission of anthropogenic GHGs (CO_2 in particular) and the degradation of air quality in urban areas [5]. Modifying the surface albedo of roofs has little co-benefit, or even causes adverse effects, on improving air quality or reducing CO_2 emissions. Thus, to improve the overall livability of urban environment, nature-based solutions, such as green roofs/walls, urban lawns, shade trees, etc. have lately emerged as a more sustainable alternative for heat mitigation and energy saving [35]. In particular, green roofs, in contrast to white/hybrid roofs, can provide cooling via evapo-transpiration during the hot season, while preventing heating penalty in the cold season through the insulation by the additional soil layer [39]. For example, it was found that green roofs had the potential to reduce the roof surface temperature by 4-12°C and lower the annual energy consumption by 2.2-16.7% [42].

The efficacy of cooling and building energy saving potentials of green roofs, in general, depends on the background climate conditions and management practices of the local cities. Moreover, in arid or semi-arid cities, it requires regular irrigation in order to maintain green roofs and their biological functions. Hence, heat mitigation using green roofs supported by urban irrigation is essentially reduced to the question "how much water does it take for cooling?" [43] that involves the heat-water trade-off. Thus, in arid and semi-arid cities, it is imperative to design and implement *smart* irrigation schemes that are capable of maximizing the total (combined) energy-water saving potential [44] of green roofs.

In past decades, tremendous effort and resources have been devoted to the study of performance of diverse roof engineering technology in terms of cooling and building energy saving. Despite that, most previous work was focused exclusively on case studies of single roof technology (e.g. white or green roofs), whereas the intercomparison of different engineering approaches in contrasting climate conditions remains scarce. In this study, we adopt a state-of-art urban canopy model (UCM) to investigate the year-long energy saving potential of different roof engineering technology, including white, hybrid, and green (vegetated with different irrigation schemes) roofs. More specifically, the model is applied to two contrasting built environments, i.e. the sub-urban area of Princeton University campus and the urban residential area in Phoenix metropolitan, to demonstrate the adaptivity and suitability of different roofs to the locality of the urban environment. We then quantify the combined monetary building energy-water saving based on the local prices of water and electricity during the study period.

2. Study Areas and Method

2.1. Study areas

In this study, we selected two contrasting urban environments, viz. the sub-urban Princeton campus and the Phoenix metropolitan area as our study areas. In addition, Princeton, New Jersey has a humid continental climate, while Phoenix, Arizona, is characterized as an arid subtropical desert climate. According to the U.S. Monthly Climate Normal (1991-2020), obtained from National Centers for Environmental Information (NECI) of the National Oceanic and Atmospheric Administration (NOAA) (https://www.ncei.noaa.gov/metadata/geoportal/rest/metadata/item/gov.noaa.ncdc:C01620/html), Princeton has an annual mean temperature of 12.3 °C and an annual precipitation of 1159.0 mm that is roughly evenly distributed in all the 12 months, while in Phoenix the annual mean temperature is as high as 24.2 °C and the annual precipitation is merely 183.4 mm.

Each study area was equipped with eddy covariance (EC) flux towers with long-term monitoring of the built environment, which facilitates the model setup and validation in subsequent analysis. The map of both study areas and the locations of the EC towers are shown in **Figure 1**. The simulation periods of both areas are an entire calendar year, in the period May 1, 2010 – April 30, 2011, for Princeton, and January 1 - December 31, 2012, for Phoenix. Moreover, located in the Sonoran Desert, Phoenix has tremendous cooling demands and irrigation water consumption (up to 70% of outdoor household water use) due to the tedious summer, while New England, where Princeton is located, has more significant demands for heating due to the temperate climate [46].

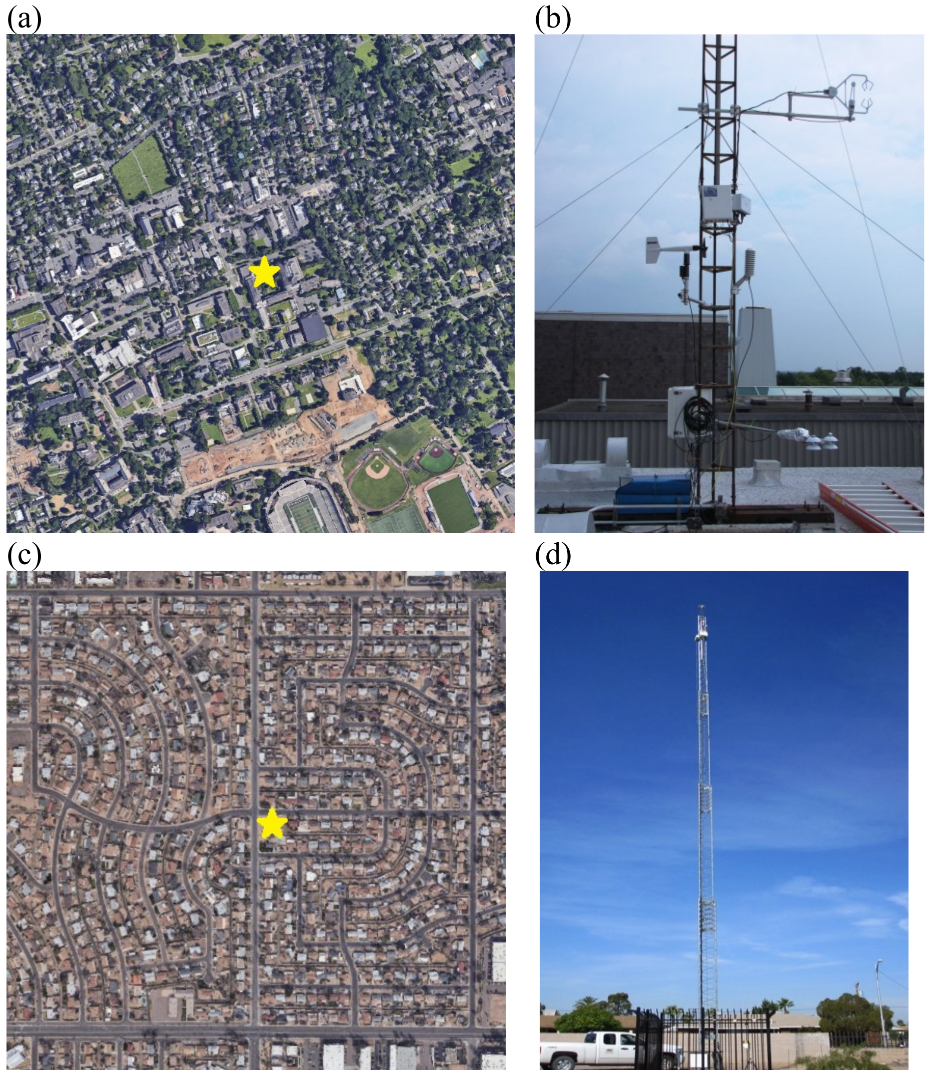

Figure 1. The study areas of Princeton: (a) the google map of Princeton University campus where (b) the eddy covariance (EC) tower (marked as yellow star) is located, and Phoenix: (c) the map of neighborhoods in West Phoenix, Arizona, with (d) the EC tower.

<u>2.2. Roof designs and irrigation schemes</u>

Located in the mid-latitudes, both Phoenix and Princeton have high seasonal variability of temperature, which induces cooling demands in summer and heating demands in winter for buildings in both areas. To realistically estimate the energy consumption of buildings with different roofs, we split the whole year into the warm and cold seasons, where only the cooling/heating demand is considered for the warm/cold season. For the Phoenix metropolitan area, the warm season is defined as the period from April 1 to October 31, while the cool season is defined as the remaining period from November 1 to March 31. For the Princeton metropolitan area, the warm season is from June 1 to August 31 and the cool season is from September 1 to May 31.

In this study, we evaluate the cooling and energy saving potentials of three different types of roofs, viz. the white, hybrid, and green roofs, in contrast to the conventional roof system, as sketched in **Figure 2**. More specifically, for the green roofs, we consider different irrigation schemes to achieve the optimal monetary saving for energy-water trade-off, which is particularly important for Phoenix as a desert city. The values of roof surface albedo and changes of soil water content per different irrigation schemes are summarized in **Table 1**. The conventional roof, which also serves the baseline scenario in this study, mainly consists of concrete and gravels with an albedo of 0.20. The white roof, with an albedo of 0.60, could lower the temperature in the whole year, and thus cut back the cooling demands in the warm season but increase the heating demands in the cool season. The hybrid roof is intended to maximize energy savings by adopting temperature-adaptive albedos for different seasons. In this study, the albedo of the hybrid roof is 0.60 in the warm season and 0.10 in the cool season, which enables the all-season reduction of both the heating and cooling demands. The green roof has more sophisticated engineering design with layered structure, including vegetation, soil, drainage, pavement, and insulation layers. The surface albedo of green roof is largely determined by the leaf area of vegetation and the soil water content, which varies irrigation amount as well as seasonal vegetation dynamics. But as the governing mechanism of green roofs as a heat mitigation strategy is evapo-transpirative cooling (rather than reflectivity), we use a fixed albedo of 0.15 for green roof in this study.

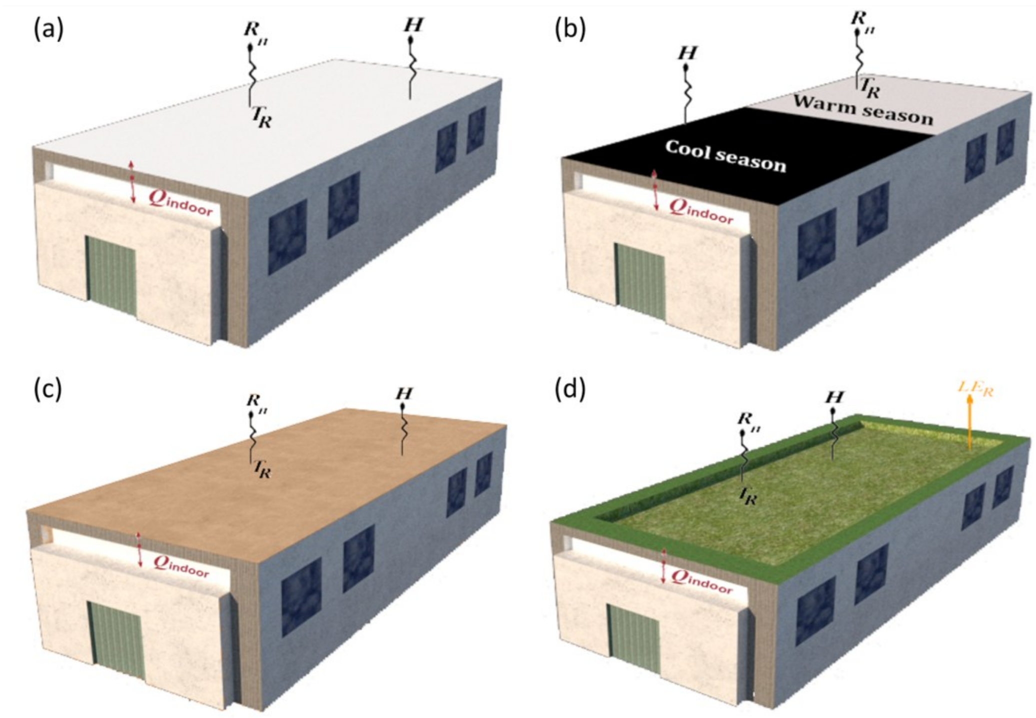

Figure 2. Schematics of different roof systems for heat mitigation: (a) white roof, (b) hybrid roof by modifying the roof surface albedo, (c) conventional roof, and (d) green roof with environmental-controlled irrigation schemes.

In addition, for the green roof system, we adopt four different irrigation schemes, which can facilitate the evapotranspiration of the vegetation and thus ameliorate the ambient thermal environment, in contrast to the baseline case (no irrigation). In Princeton, the vegetation in the green roof can survive without irrigation in the monsoon season due to the plenty precipitation. In Phoenix, on the contrary, the soil moisture will fall below the wilting point without irrigation due to the inadequate precipitation, which only allows the growth of limited species of arid and semi-arid vegetation. For consistency, we use the same irrigation schemes for both study areas.

Table 1. The albedos of different roof types and irrigation amount of five irrigation schemes

Roof type	**Roof code**	Albedo a (-)
Conventional roof	CR	0.20
White roof	WR	0.60
Hybrid roof	HR	0.60 (warm season), 0.10 (cool season)
Green roof	GR	0.15
Irrigation schemes	**Irrigation scheme code**	Irrigation amount in terms of the increase of volumetric water content (cm^3 cm^{-3}) of the top (10-cm) soil layer
No irrigation (baseline)	GR0	0
Moisture-controlled I	GR1	0.1, $\theta_{threshold} = 0.15$
Moisture-controlled II	GR2	0.1, $\theta_{threshold} = 0.24$
Daily constant	GR3	Vary monthly, per city's guidance
Flood irrigation	GR4	Fully saturated with ponding water depth of 2 cm (in the warm season) or 1 cm (in the cool season)

The first two schemes are both soil moisture-controlled but with different threshold of soil water content $\theta_{threshold}$ (at which irrigation is activated) of 0.15 (moisture-controlled Scheme I) and 0.24 (Scheme II), respectively. These values are determined based on the observational and modeling results for several different xeric (Phoenix) and mesic (Princeton) landscapes in Phoenix metropolitan, where the wilting points range from 0.15 to 0.24 [47]. Thus, we set $\theta_{threshold} = 0.15$ and 0.24 for soil moisture-controlled irrigation Scheme I and II, respectively, to maintain the topsoil moisture above the wilting point. Irrigation is activated when the top-soil water content drops below these threshold values and stops when the top-soil (10-cm) water content increases by 10% (0.1 cm^3 cm^{-3}) to adequately support the biological functions of vegetated green roofs. The third is a daily constant irrigation scheme that is automated to operate at 9 pm LST. The daily irrigation amount of this scheme is estimated by the *in-situ* measurement of the monthly total outdoor irrigation water use [48], divided by number of days in the month.

The last scheme is the flood irrigation of urban vegetation, applied weekly or biweekly at 9 pm LST during the warm or cool seasons, respectively. Flood irrigation is still widely used in old neighborhood in Phoenix, which results in the saturation of the top-soil layer and water ponding immediately after the irrigation. Per field observation, the ponding water depth is estimated to be 2 cm and 1 cm during the warm and cool seasons, respectively.

2.3. Modeling urban land surface processes

In this study, we adopt a state-of-the-art urban land surface model, namely, the Arizona Single-Layer Urban canopy Model (ASLUM) that has been developed and continuously improved over past decades [49]. ASLUM realistically resolves the physics of land surface processes in the urban canopy layer (UCL), including the transport of heat, moisture, and scalar quantities (e.g., carbon dioxide) over built terrains. In particular, the model incorporates urban vegetation dynamics, the green roof system in particular, and urban hydrological processes that have been tested and extensively applied to study the impact of various urban heat mitigation strategies in diverse urban environments [33]. According to a recent global intercomparison of 30 urban land surface models in the Urban-PLUMBER project, ASLUM (v2.0 and v3.0) were both among the best, based on their numerical performance [57].

The surface energy balance that drives the heat transport in the UCL is given by,

$$R_n = H + LE + G_0, \quad (1)$$

where H, LE and G_0 are anthropogenic, sensible, latent, and ground soil heat fluxes, respectively, and R_n is the net radiation as the sum of radiative components,

$$R_n = S_{\text{net}} + L_{\text{net}} = \left(S_{\text{down}} - S_{\text{up}}\right) + \left(L_{\text{down}} - L_{\text{up}}\right), \quad (2)$$

with S and L the shortwave and longwave radiation, and subscripts 'down' and 'up' standing for upwelling and downwelling direction, respectively. At the roof level, the net shortwave radiation is calculated as,

$$S_{\text{net}} = (1-a)(S_D + S_Q), \tag{3}$$

where S_D and S_Q are the measured direct and the diffuse solar radiation received by a horizontal surface respectively, and a is the surface albedo. The net longwave radiation is given by,

$$L_{\text{net}} = L_{\text{down}} - \varepsilon\sigma T_R^4, \tag{4}$$

where ε is the emissivity, σ is the Stefan–Boltzmann constant, and T_R is the roof surface temperature.

The profile (vertical distribution) of roof temperatures and soil heat fluxes are obtained by solving the one-dimensional (1D) heat conduction equation analytically using Green's function approach [49], as

$$T(z,t) = T_0 + \int_0^t f_1(t-\tau)dg(z,\tau) - \int_0^t f_2(t-\tau)dg(d-z,\tau) \tag{5}$$

$$G(z,t) = -k\frac{\partial T}{\partial z} = -k[\int_0^t f_1(t-\tau)dg'(z,\tau) - \int_0^t f_2(t-\tau)dg'(d-z,\tau)] \tag{6}$$

where z is the depth from the roof surface (positive downward), k is the thermal conductivity, f_1 and f_2 are the heat fluxes at the exterior (exposed to sun) and interior boundaries of the roofs, respectively, T_0 is the initial temperature profile inside the solid which is assumed to be uniform), $g(z, t)$ is the fundamental (Green's function) solution of 1D heat diffusion with homogeneous boundary conditions, and $g' = \partial g / \partial z$ is the spatial derivative of g. In particular, the surface (skin) temperature of different roofs can be obtained by setting $z = 0$, viz. $T_R = T(0, t)$.

The turbulent transport of heat from rooftop to the atmosphere, including sensible heat flux and latent hear fluxes, are calculated as follows,

$$H = \frac{c_p \rho_a (T_R - T_a)}{r_a}, \tag{7}$$

$$LE = \beta_e \frac{L_v \rho_a (q_R^* - q_a)}{r_a}, \tag{8}$$

where c_p, ρ_a, and T_a are the specific heat, density, and temperature of air, r_a is the aerodynamic resistance, L_v is the latent heat of vaporization, q is the specific humidity, the superscript star stands for saturation, and β_e is a reduction factor for non-saturated surface as a function of soil-water content, which can be approximated as [58],

$$\beta_e = \frac{\theta - \theta_r}{\theta_s - \theta_r}, \tag{9}$$

where θ is the volumetric soil water content, θ_s the soil-water content at saturation and θ_r the soil-water content at which evaporation is suppressed.

3. Results and Discussion

3.1. Model validation

We first evaluate the model performance for the baseline cases in Phoenix and Princeton, respectively. The annual *in situ* datasets at the two study areas were measured by the EC tower deployed at Princeton University campus (**Fig. 1c**) during May 1, 2010 – April 30, 2011, and Maryvale, West Phoenix (**Fig. 1d**) throughout January 1 - December 31, 2012, respectively. The results of comparisons of predicted and measured roof surface temperatures (T_R) and net radiation (R_n) are shown as scatter plots in **Figure 3**. For the entire simulation period, the root mean square errors (RMSE) are 1.50 °C and 2.09 °C for T_R in Phoenix and Princeton, respectively, and 13.43 W m^{-2} and 19.27 W m^{-2} for R_n in Phoenix and Princeton, respectively. The values of coefficient of determination, R^2, as a fitted curve of the scatters, are 0.9781, 0.9215, 0.9643, 0.8398, of the four subplots in **Fig. 3**, respectively. The results indicate that the predictions of ASLUM agree reasonably well with the field observations. The model performance is in general better in the arid environment under clear conditions, as the presence of clouds and precipitations complicates the heat-moisture interactions, thus leading to reduced accuracy of model predictions.

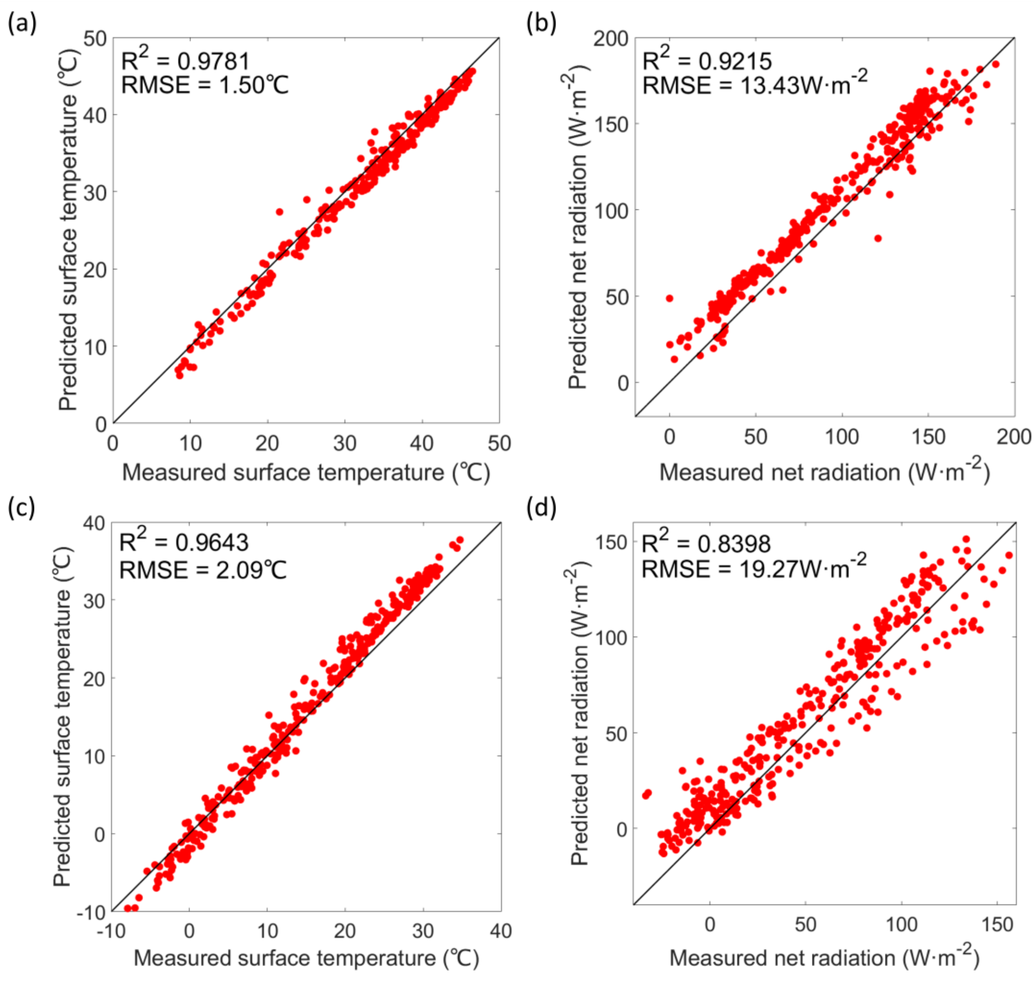

Figure 3. Comparisons of predicted and measured (a) T_R and (b) R_n in Phoenix, and (c) T_R and (d) R_n in Princeton.

<u>3.2. The impact on roof thermal performance</u>

In this study, the surface albedo of white and hybrid roofs and irrigation schemes of green roofs are two main factors that modify the thermal performance of roofs. **Figures 4** and **5** show the thermal responses of different roof systems to the change of these parameters (Table 1), including the changes of roof surface temperature (T_R), net radiation (R_n), sensible heat (H), and latent heat (LE), with respect to those of the conventional roof (baseline), in Phoenix and Princeton, respectively. We find that in both areas, the white roof and green roofs with irrigation have the cooling effect throughout the year. In contrast, the hybrid roof reduces roof temperature during the warm season but has a warming effect in the cool season due to surface darkening, thus effectively avoid heating penalty.

In Phoenix, as shown in **Fig. 4**, the green roof without irrigation induces a warming effect on roof surface temperature due to the lower albedo (0.15) than that of the conventional roof (0.20). From May to September, green roofs in Phoenix with flood irrigation and daily constant irrigation has the most significant cooling effects, which has the maximum reduction in T_R of 11.1°C in late June; the moisture-controlled scheme II induces a larger roof surface reduction than the moisture-controlled scheme I due to the higher moisture threshold and thus a larger irrigation amount. From October to April, the white roof cools the roof surface most, while the reductions in roof surface temperatures of green roof are less significant than in summer, especially in December and January. The surface cooling of green roofs with adequate irrigation is directly related to the evapotranspiration of vegetation, which is controlled by the supply of available energy ($R_n – H – LE$) impinged on the roof surface. Therefore, the green roof with irrigation has a better cooling capability in summer when stronger solar radiation exists. The changes of R_n on roofs without irrigation (in comparison to the conventional roof) (**Fig. 4b**), i.e., white roof, hybrid roof, and non-irrigated green roof, are nearly identical to those of the surface temperature (**Fig. 4a**).

Furthermore, green roofs in Phoenix with irrigation induce increases in the net radiation, which is especially significant in summer. This is primarily because the strong surface cooling induced by irrigated green roofs, in turn, results in the reduced upwelling longwave radiation, as well as the decreased sensible heat, which outweighs the increase in latent heat due to evapotranspiration. For the white roof, the net shortwave radiation decreases due to higher shortwave reflectivity and thus causes the reduction in the total net radiation. Likewise, the dominant effect of albedo causes a slight increase of net radiation due to roof darkening in the cool season and the same trend as the white roof in the warm season. Sensible heat flux, on the other hand, is strongly regulated by the surface temperature, thus its changes (**Fig. 4c**) are very similar to that of the surface temperature (**Fig. 4a**). For the latent heat flux arising from the roof surfaces, all green roofs with irrigation induce increase of the latent heat flux, which is more significant in summer than in winter due to the stronger evapotranspiration in summer. There is slight (and very sporadic) increase of latent heat on the green roof without irrigation, which is due to evaporation of scarce natural precipitation in Phoenix.

There are some noticeable differences between the thermal performances in Phoenix and Princeton. First, the shorter duration of warm season in Princeton is responsible for the lesser cooling effect of white and hybrid roofs, and the total energy-water trade-off (detailed in Section 4.3 below). In addition, as shown in **Figure 5**, the thermal behavior of green roofs with no irrigation and moisture-controlled scheme I (limited irrigation above wilting point) are nearly the same. This is because that the precipitation in Princeton is sufficient to keep the soil water content of green roofs above the lower limit of wilting point ($\theta_{\text{threshold}} = 0.15$) throughout the year. For the same reason, green roof without irrigation does not exhibit a warming effect in Princeton (**Fig. 5a**) in comparison to that in Phoenix (**Fig. 4a**).

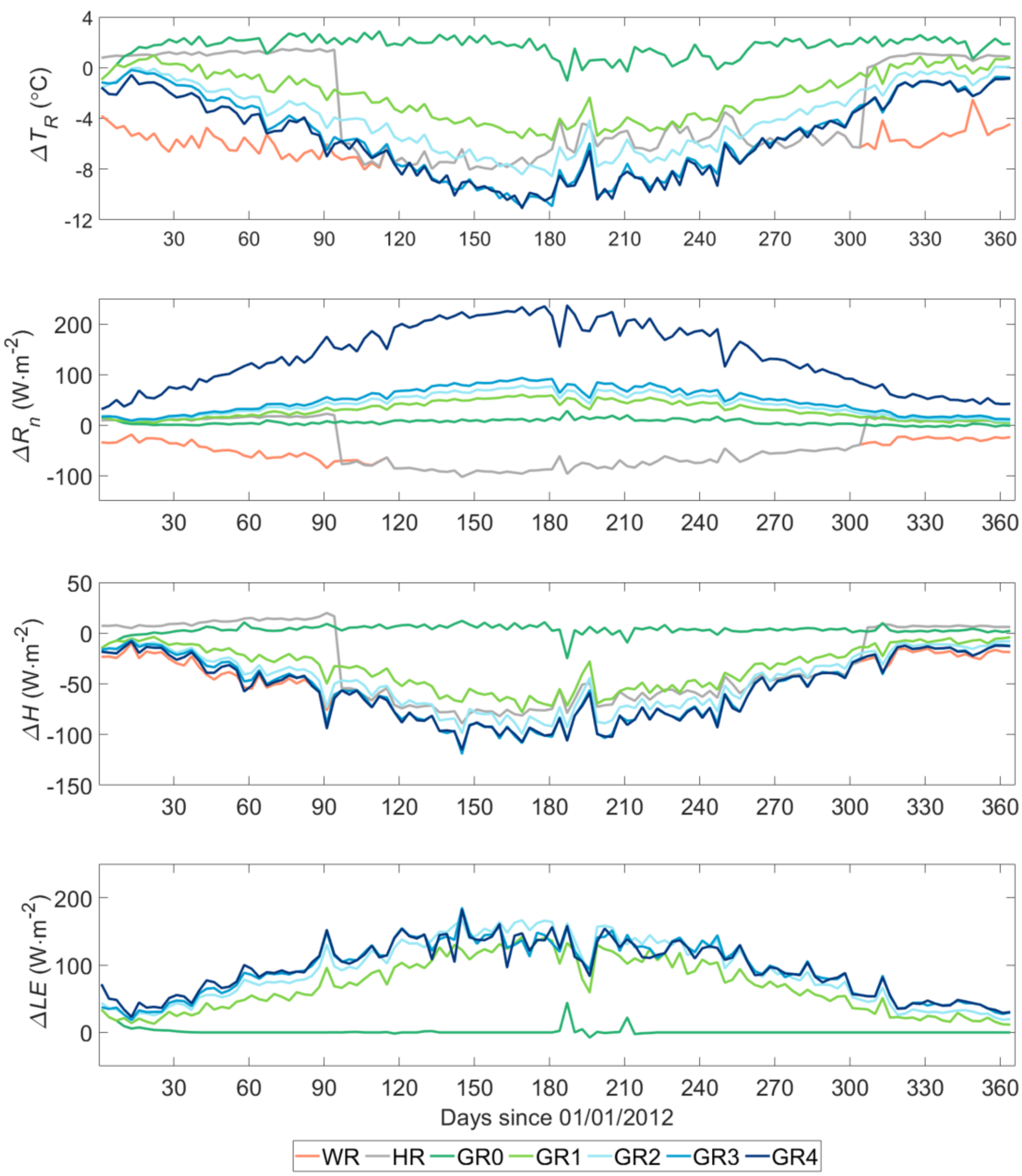

Figure 4. 3-day averaged changes of the thermal performance of different roofs in Phoenix, in comparison to the conventional roof (baseline case), including changes of (a) roof temperature ΔT_R, (b) net radiation ΔR_n, (c) sensible heat ΔH, and (d) latent heat ΔLE.

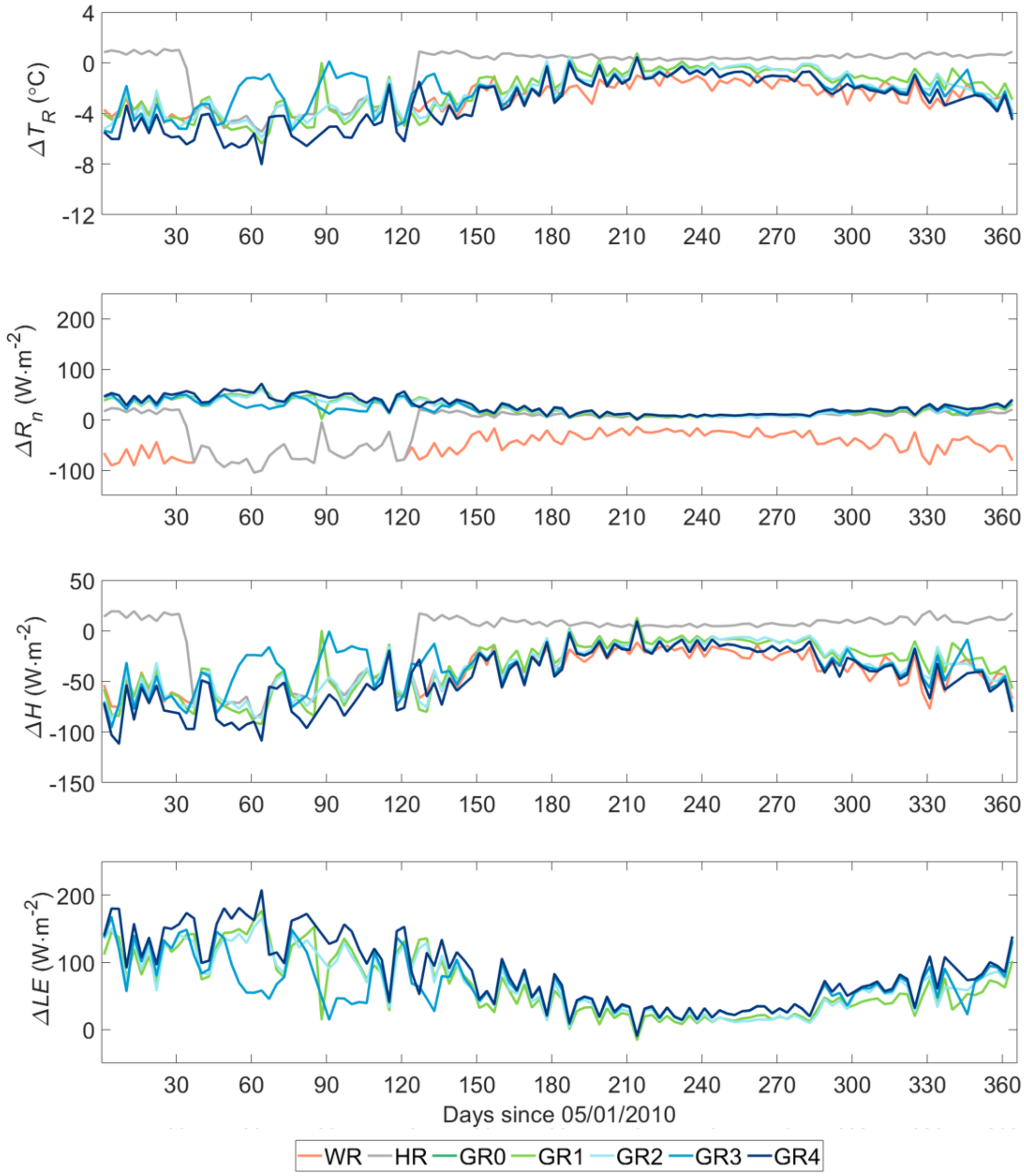

Figure 5. Same as Figure 4, but in the study area of Princeton.

<u>3.3. The impact on energy-water trade-off and combined saving</u>

In this study, we focus on the building energy consumption by heating and air conditioning (HAC) systems as they are directly related to the indoor thermal response to outdoor thermal environment through roofs. For simplicity, we use the conductive heat flux, computed by Eq. (6), to estimate the required HAC load in order to maintain a constant indoor temperature of 24 °C. Note that though there are occasions when the indoor temperature may drop below the threshold during the warm season (e.g., a cool summer night in Princeton), indoor heating is not activated considering the customary working mechanism of air conditioning systems, likewise for cooling need during the cool season. Thus, in this study, we take consideration of cooling demand in the warm season and heating demand in the cool season exclusively for both study areas. In addition, the water consumption is considered for green roofs with irrigation based on the amount of irrigation water use.

Table 2 The unit prices of electricity and water in Phoenix and Princeton

Study area	Phoenix	Princeton
Average price of electricity (¢ kWh^{-1})	11.31	14.80
Price of water (\$ m^{-3})		
January	1.49	2.05
February	1.49	2.05
March	1.49	2.05
April	1.70	2.05
May	1.70	2.05
June	1.86	2.05
July	1.86	2.05
August	1.86	2.05
September	1.86	2.05
October	1.70	2.05
November	1.70	2.05
December	1.49	2.05

The resultant *total* cost per unit roof area (\$ m^{-2}) of combined energy (electricity) and water consumption is therefore given by,

$$\mathrm{Cost}_{\mathrm{total}} = P_{\mathrm{water}} V_{\mathrm{water}} + P_{\mathrm{electricity}} \sum_t Q_{\mathrm{indoor}} \,, \tag{10}$$

where P_{water} and $P_{\mathrm{electricity}}$ are the unit prices of water (per m^3) and electricity (per kWh) respectively, V_{water} is the irrigation amount per unit area ($m^3\ m^{-2}$), Q_{indoor} is the model predicted indoor heat flux through the roof (kW m^{-2}) [44]. The total cost is in dollar per square meter roof area. As shown in **Table 2**, The average electricity rate of Arizona and New Jersey is obtained from the report of U.S. Energy Information Administration (https://www.eia.gov/electricity/state/); The water prices in Phoenix and Princeton are acquired from the city of Phoenix (https://www.phoenix.gov/waterservices/customerservices/rateinfo) and New Jersey American Water (https://www.amwater.com/njaw/) respectively. The combined *savings* per unit roof area (\$ m^{-2}) of different roof systems are calculated as the difference between the total cost of a given roof and that of the conventional roof.

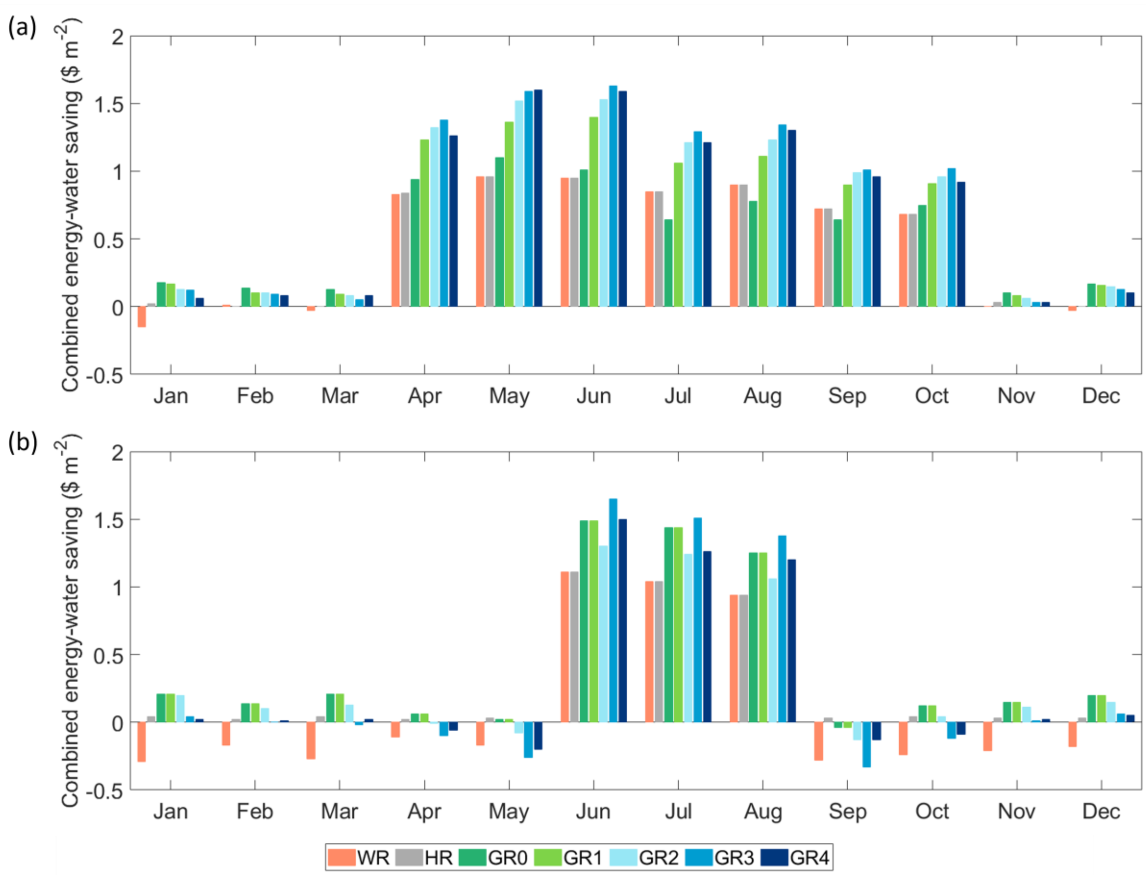

Figure 6. The results of monthly savings of different roof types and irrigation schemes in (a) Phoenix and (b) Princeton, in comparison to the conventional roof.

The monthly combined energy-water savings of different roofs and irrigation schemes, as compared to the conventional roof, in Phoenix and Princeton are presented in **Figure 6**. In both study areas, since the white roof has cooling effects in the whole year, it increases the energy consumption in the cool season (the heating penalty) and reduce energy consumption in the warm season. The hybrid roof, on the other hand, can successfully avoid the heating penalty, and achieves positive savings in all seasons. Some of the irrigation schemes, especially flood irrigation and daily constant irrigation, lead to increased consumption in April, May, September, and October in Princeton. Except for the aforementioned cases, all the roofs reduce the total costs, which are more significant in summer. In Phoenix, in particular, the maximum monthly saving in the cool season is generated by the green roof without irrigation since its warming effects as no water demand is needed. Irrigated green roofs have savings higher than roofs without irrigation in the warm season, leading to a maximum saving of \$1.63 m^{-2} by green roofs with daily constant irrigation in June. In Princeton, the green roof with no irrigation has the same monthly savings as moisture-controlled scheme I, resulting in maximum saving in the cool season. In the warm season, green roofs with daily constant irrigation attain the maximum saving, up to \$1.65 m^{-2} in July.

The total annual savings of different roofs and irrigation schemes in Phoenix and Princeton are shown in **Figure 7**. The least annual savings are attributed to the white roof in both study areas, amounting to \$5.70 m^{-2} and \$1.17 m^{-2} in Phoenix and Princeton, respectively. In Phoenix, the maximum annual saving is \$9.68 m^{-2}, from green roofs with moisture-controlled scheme II due to the significant cooling effects in the warm season but controlled use of irrigation water. In Princeton, the maximum total annual saving is \$5.23 m^{-2}, resulted from the use green roof with no irrigation (by natural precipitation). The sufficient precipitation in Princeton enables the vegetation on the green roof to keep enough moisture needed for the biological functions and evapotranspiration of the vegetation. Therefore, green roofs in Princeton is able to achieve significant cooling effects without minimal irrigation need.

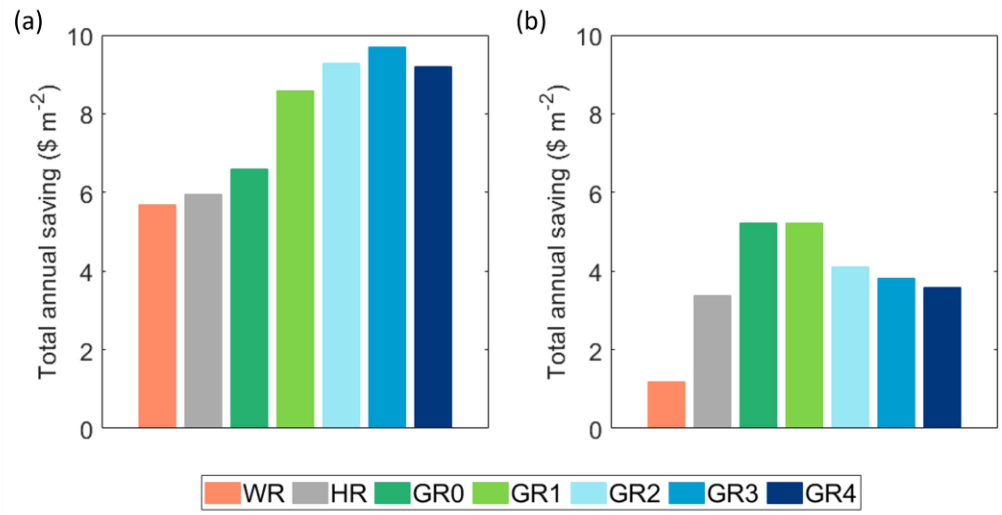

Figure 7. The results of annual savings of different roof types and irrigation schemes in (a) Phoenix and (b) Princeton, in comparison to the conventional roof.

<u>3.4. Sensitivity of energy savings to coefficient of performance</u>

In this study, the heating and cooling systems are implicitly assumed to response spontaneously to incident heat fluxes into the building through roofs to maintain a constant indoor temperature of 24 ºC. To quantify the impact of thermodynamic coefficient of performance (COP) on the overall annual savings, we calculated the total annual savings of all roof types and irrigation schemes in Phoenix and Princeton corresponding to the COP values. The results are shown in **Figure 8**. To analyze the sensitivity of total savings to COP, we select the values from 1 to 10 that could cover the common interval (from 2 to 4) in practical applications [59]. Since with the improvement of COP, the electricity consumed by the HAC system to transfer the same amount of heat decreases, the differences of the electricity consumption among different roofs and irrigation schemes reduce and thus result in lowered savings. Total savings of roofs with irrigation decreases faster with COP than roofs without irrigation. It is notable that the savings of green roofs with irrigation will be negative when COP is higher than a certain threshold (5.83 in Phoenix and 2.49 in Princeton), resulting from the reduced savings of electricity that cannot compensate the water consumption.

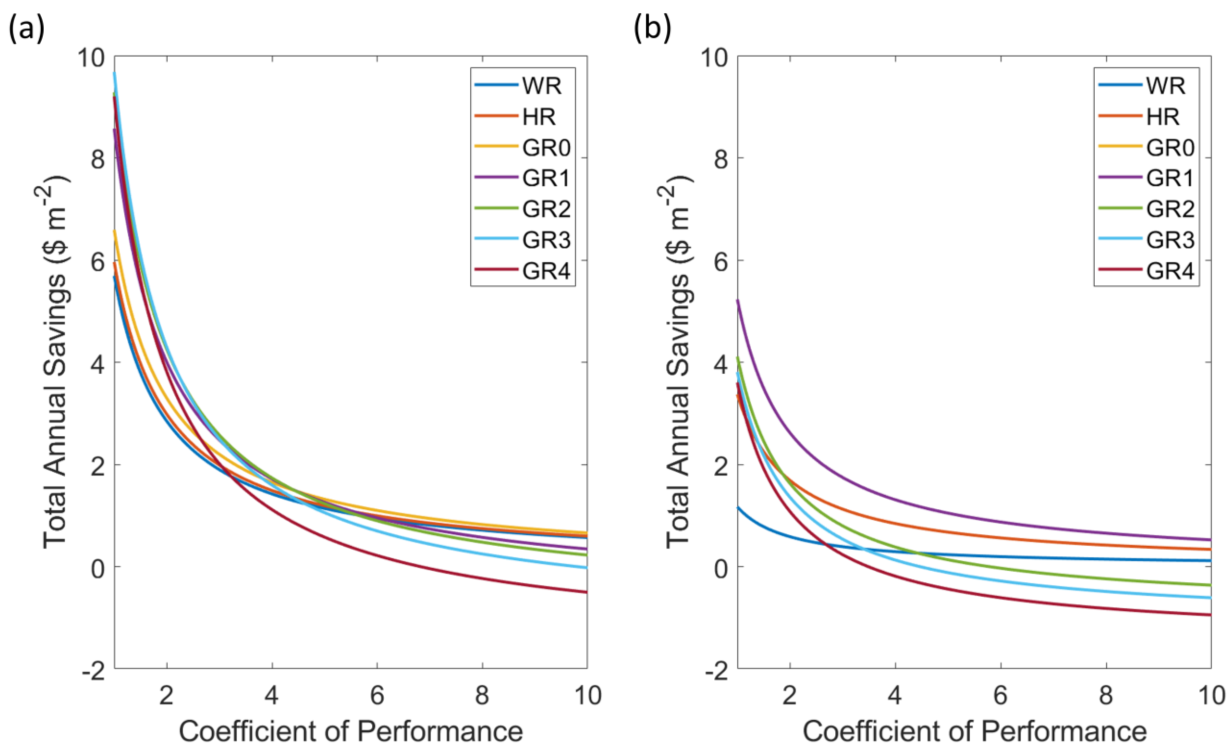

Figure 8. The changes of annual savings of different roof types and irrigation schemes in (a) Phoenix and (b) Princeton versus COP (scaled from 1 to 10).

4. Concluding Remarks

In this study, we used a state-of-the-art urban land surface model, i.e., ASLUM to evaluate the potential of diverse roof systems for ameliorating the thermal environment and improving the efficiency of building energy-water trade-off in two contrasting built environments. Though both white roofs (aka "cool" roofs) and green roofs (aka "eco-roofs") are popular heat mitigating strategies that are widely adopted by urban planners and practitioners, it was found that the nature-based solution, i.e., green roofs, are the preferred heat mitigation in both arid metropolitan and temperate sub-urban areas (**Fig. 7**). Despite the fact that the use of irrigation for green roofs incurs additional cost of water consumption, this water use can be strategically controlled to yield optimal heat-water trade-off and maximize the combined energy-water savings. With the assumption of spontaneous response of HAC systems, the maximum total annual savings of the green roof can be up to \$9.68 m^{-2} and 5.23 m^{-2}, in Phoenix and Princeton respectively. In climate regions with sufficient precipitation, the advantage of green roofs is more manifest as the use of irrigation water can be further reduced. The total annual saving is more prominent in the arid city of Phoenix (vary from \$5.70 m^{-2} to \$9.68 m^{-2}) than the sub-urban Princeton town (vary from \$1.17 m^{-2} to \$5.23 m^{-2}), as the former experiences more severe UHI and thus has more potential for heat mitigation and building energy saving. The use of hybrid roofs with reduced albedo in cool seasons helps to avoid the heating penalty incurred by pure white roofs; the difference is more prominent in Princeton (\$2.20 m^{-2}) where a temperate climate and long cool seasons requires substantial heating demand. The results of this study are informative to homeowners and urban planners in selecting the optimal solutions to heat mitigation and building energy saving and then further alleviate energy shortages in this era with increasing energy demands, especially in the areas with higher temperatures and less precipitation. According to the results, in the contiguous United States, green roofs without irrigation is an ideal solution to energy saving in areas with sufficient precipitation, viz. the regions of humid continental and humid subtropical climate located to the east of the Rocky Mountains; while in the Rocky Mountains area, where precipitation is much less, more irrigation is needed to sustain the green roofs.

However, there are a few caveats of the method used in this study. First, the estimate of building energy consumption by HAC systems and the amount of irrigation water are based on a number of simplified assumptions, including, constant indoor temperature, exact balance of indoor heat fluxes by HAC systems, instantons increase of soil water content by irrigation, no vegetation dynamics, etc. Thus, the values of estimated savings should not be taken as quantitatively exact, but rather qualitatively informative. Secondly, to maintain the consistency in intercomparison of different scenarios, we decoupled the urban land-atmosphere interactions in our numerical modeling, so that the cooling of roof surface has no feedback to the ambient air temperature. In addition, we performed the numerical experiments in an annual cycle of a particular year in each study area, thus the results are subject to the influence of particular hydrometeorological conditions, especially the amount of precipitation on the demand of irrigation water use (Phoenix in particular). Thus, the presence of hydroclimatic extremes, e.g., heatwaves or extreme droughts, could be decisive in modifying the building energy as well as urban water use patterns.

Nevertheless, the proposed modeling method in this study can be used to guide future work to improve the quantification of the trade-off between building energy and water irrigation for green roofs to estimate more accurate saving potential. Such improvements can be developed by including: (1) more sophisticated building energy models to the urban canopy layer physics, (2) urban vegetation dynamics (e.g. growth and wilting) and land-atmosphere feedback, (3) life cycle analysis of different roof systems (e.g., cost of implementation and maintenance of roof vegetation and pavement albedo) and secondary energy-water nexus (e.g., energy to transport irrigation water), and (4) the impact of regional climate change, especially the presence of hydroclimate extremes on different roof systems and their performance. The current study can also be readily extended to other cities in the U.S. or worldwide. The key factors determining the building energy efficiency in different cities are diverse, including, for example, the local urban microclimate, prices and accessibility of different forms of energy (e.g. fossil fuels, electricity, renewable energy, etc.) and water resources, or even the preference of residents in cities (e.g. vegetated versus painted roofs), to name a few. It is also important to note that if energy-water-saving roof systems are to be adopted in massive scales in the built environment, especially those in close spatial proximity to mega cities (i.e., urban clustering [60]), the effect might be influencing one another [61, 62] due to cross-regional atmospheric transport in complex urban climate networks. Quantification of the energy saving potential in different cities with mutual side effect or co-benefit will, therefore, be informative to urban planners for their selection of fitful roof systems for heat mitigation with desirable cost-saving benefits.

Acknowledgement

This study is supported by the U. S. National Science Foundation (NSF) under Grant No. AGS-2300548, Arizona Board of Regents (ABOR) under the project "Smart Tree Watering in Arizona's Urban Environment", and Arizona State University-Salt River Project Joint Research Project.

References:

[1] Department of Economic and Social Affairs, United Nations. (2019). Urban and rural population growth and world urbanization prospects. World Urbanization Prospects: The 2018 Revision, New York, NY, United States of America, 9.

[2] The United Nations Human Settlements Programme, United Nations. (2020). The Value of Sustainable Urbanization, United Nations Human Settlements Programme. *World Cities Report 2020,* Nairobi, Kenya, 377.

[3] Antognelli, S., and Vizzari, M. (2016). Ecosystem and urban services for landscape livability: A model for quantification of stakeholders' perceived importance. *Land Use Policy*, 50, 277-292.

[4] Kumar, P., Druckman, A., Gallagher, J., Gatersleben, B., Allison, S., Eisenman, T.S., et al. (2019). The nexus between air pollution, green infrastructure and human health. *Environment International*, 133, 105181.

[5] Wang, C., Li, Q., and Wang, Z.H. (2018). Quantifying the impact of urban trees on passive pollutant dispersion using a coupled large-eddy simulation-Lagrangian stochastic model. *Building and Environment*, 145, 33-49.

[6] Oke, T.R. (1967). City size and the urban heat island. *Atmospheric Environment*, 7, 769-779.

[7] Oke, T.R. (1982). The energetic basis of the urban heat island. *Quarterly Journal of the Royal Meteorological Society*, 108(455), 1-24.

[8] Wang, Z.H. (2022). Reconceptualizing urban heat island: Beyond the urban-rural dichotomy. *Sustainable Cities and Society*, 77, 103581.

[9] Zinzi, M., Carnielo, E., and Mattoni, B. (2018). On the relation between urban climate and energy performance of buildings. A three-years experience in Rome, Italy. *Applied Energy*,

221, 148-160.

[10] Yang, X., Peng, L.L.H., Jiang, Z., Chen, Y., Yao, L., He, Y., et al. (2020). Impact of urban heat island on energy demand in buildings: Local climate zones in Nanjing. *Applied Energy*, 260, 114279.

[11] Li, X., Zhou, Y., Yu, S., Jia, G., Li, H., Li, W. (2019). Urban heat island impacts on building energy consumption: A review of approaches and findings. *Energy*, 174, 407-419.

[12] Kang, J.N., Wei, Y.M., Liu, L.C., Han, R., Yu, B.Y., and Wang, J.W. (2020). Energy systems for climate change mitigation: A systematic review. *Applied Energy*, 263, 114602.

[13] Wang, Y., Yang, X., and Wang, Z.H. (2024), Causal mediation of urban temperature by geopotential height in U.S. cities, *Sustainable Cities and Society*, 100, 105010.

[14] Hou, H., Longyang, Q., Su, H., Zeng, R., Xu, T., and Wang, Z.H. (2023). Prioritizing environmental determinants of urban heat islands: A machine learning study for major cities in China. *International Journal of Applied Earth Observation and Geoinformation*, 122, 103411.

[15] Akbari, H., and Rose, L.S. (2008). Urban surfaces and heat island mitigation potentials. *Journal of Human–Environment System*, 11(2), 85–101.

[16] Xu, T.F., Sathaye, J., Akbari, H., Garg, V., and Tetali, S. (2012). Quantifying the direct benefits of cool roofs in an urban setting: Reduced cooling energy use and lowered greenhouse gas emissions. *Building and Environment*, 48, 1-6.

[17] Baniassadi, A., Sailor, D.J., and Ban-Weiss, G.A. (2019). Potential energy and climate benefits of super-cool materials as a rooftop strategy. *Urban Climate*, 29, 100495.

[18] Wang, C., Wang, Z.H., Kaloush, K.E., and Shacat, J. (2021a). Cool pavements for urban heat island mitigation: A synthetic review. *Renewable & Sustainable Energy Reviews*, 146,

111171.

[19] Testa, J., and Krarti, M. (2017). Evaluation of energy savings potential of variable reflective roofing systems for US buildings. *Sustainable Cities and Society*, 31, 62–73.

[20] Yang, J., Wang, Z.H., and Kaloush, K.E. (2015a). Environmental impacts of reflective materials: Is high albedo a 'silver bullet' for mitigating urban heat island? *Renewable and Sustainable Energy Reviews*, 47, 830-843.

[21] He, Y., Yu, H., Ozaki, A., and Dong, N. (2020). Thermal and energy performance of green roof and cool roof: A comparison study in Shanghai area. *Journal of Cleaner Production*, 267, 122205.

[22] Wang, Z.H. (2021). Compound environmental impact of urban mitigation strategies: Co-benefits, trade-offs, and unintended consequence. *Sustainable Cities and Society*, 75, 103284.

[23] Ramamurthy, P., Bou-Zeid, E., Smith, J., Wang, Z., Baeck, M., Hom, J., et al. (2014). Influence of sub-facet heterogeneity and material properties on the urban surface energy budget. *Journal of Applied Meteorology and Climatology*, 53(9), 2114-2129.

[24] Morin, F.J. (1959). Oxides which show a metal-to-insulator transition at the Neel temperature. *Physical review letters*, 3(1), 34-36.

[25] Tian, D., Zhang, J., and Gao, Z. (2023). The advancement of research in cool roof: super cool roof, temperature-adaptive roof and crucial issues of application in cities. *Energy and Buildings*, 291, 113131.

[26] Kim, C., Shin, J., and Ozaki, H. (2007). Effect of W doping in metal–insulator transition material VO2 by tunnelling spectroscopy. *Journal of Physics: Condensed Matter*, 19(9), 096007.

[27] Zhao, D., Aili, A., Zhai, Y., Xu, S., Tan, G., Yin, X., and Yang, R. (2019). Radiative sky cooling: Fundamental principles, materials, and applications. *Applied Physics Reviews*, 6(2), 021306.

[28] Ono, M., Chen, K., Li, W., and Fan, S. (2018). Self-adaptive radiative cooling based on phase change materials. *Optics express*, 26(18), A777-A787.

[29] Park, B., and Krarti, M. (2016). Energy performance analysis of variable reflectivity envelope systems for commercial buildings. *Energy and Buildings*, 124, 88-98.

[30] Chai, J., Chen, J., Kang, Z., Lu, L., Tang, C., and Fan, J. (2023). Temperature-adaptive rooftop covering with synergetic modulation of solar and thermal radiation for maximal energy saving. *Iscience*, 26(8), 107388.

[31] Li, P., and Wang, Z.H. (2021). Environmental co-benefits of urban greening for mitigating heat and carbon emissions. *Journal of Environmental Management*, 293, 112963.

[32] Li, P., Xu, T., Wei, S., and Wang, Z.H. (2022). Multi-objective optimization of urban environmental system design using machine learning. *Computers, Environment and Urban Systems*, 94, 101796.

[33] Li, P., Wang, Z.-H., and Wang, C. (2024), The potential of urban irrigation for counteracting carbon-climate feedback, *Nature Communications*, 15(1), 2437.

[34] Yang, X., Li, P., and Wang, Z.H. (2023). The impact of urban irrigation on the temperature-carbon feedback in U.S. cities. *Journal of Environmental Management*, 344, 118452.

[35] Sun, T., Bou-Zeid, E., Wang, Z.H., Zerba, E., and Ni, G.H. (2013). Hydrometeorological determinants of green roof performance via a vertically-resolved model for heat and water transport. *Building and Environment*, 60, 211-224.

[36] Song, J., and Wang, Z.H. (2015a). Impacts of mesic and xeric urban vegetation on outdoor

thermal comfort and microclimate in Phoenix, AZ. *Building and Environment*, 94(2), 558-568.

[37] Wang, Z.H., Zhao, X., Yang, J., and Song, J. (2016). Cooling and energy saving potentials of shade trees and urban lawns in a desert city. *Applied Energy*, 161(3), 437-444.

[38] Upreti, R., Wang, Z.H., and Yang, J. (2017). Radiative shading effect of urban trees on cooling the regional built environment. *Urban Forestry & Urban Greening*, 26, 18-24.

[39] Dvorak, B., and Volder, A. (2010). Green roof vegetation for North American ecoregions: a literature review. *Landscape and urban planning*, 96(4), 197-213.

[40] Manso, M., Teotonio, I., Silva, C.M., and Cruz, C.O. (2021). Green roof and green wall benefits and costs: A review of the quantitative evidence. *Renewable and Sustainable Energy Reviews*, 135, 110111.

[41] Mihalakakou, G., Souliotis, M., Papadaki, M., Menounou, P., Dimopoulos, P., Kolokotsa, D., et al. (2023). Green roofs as a nature-based solution for improving urban sustainability: Progress and perspectives. *Renewable and Sustainable Energy Reviews*, 180, 113306.

[42] Rawat, M., and Singh, R.N. (2022). A study on the comparative review of cool roof thermal performance in various regions. *Energy and Built Environment*, 3(3), 327-347.

[43] Gober, P., Brazel, A., Quay, R., Myint, S., Grossman-Clarke, S., Miller, A., et al. (2010). Using watered landscapes to manipulate urban heat island effects: How much water will it take to cool Phoenix? *Journal of the American Planning Association*, 76(1), 109-121.

[44] Yang, J., and Wang, Z.H. (2015). Optimizing urban irrigation schemes for the trade-off between energy and water consumption. *Energy and Buildings*, 107, 335-344.

[45] Wang, C., Wang, Z.H., and Yang, J. (2019). Urban water capacity: Irrigation for heat mitigation. *Computers, Environment and Urban Systems*, 78, 101397.

[46] Sivak, M. (2008). Where to live in the United States: combined energy demand for heating and cooling in the 50 largest metropolitan areas. *Cities*, 25(6), 396-398.

[47] Volo, T.J., Vivoni, E.R., Martin, C.A., Earl, S., and Ruddell, B.L. (2014). Modelling soil moisture, water partitioning, and plant water stress under irrigated conditions in desert urban areas. *Ecohydrology*, 7(5), 1297-1313.

[48] Martin, C. A., and Stabler, L.B. (2002). Plant gas exchange and water status in urban desert landscapes. *Journal of Arid Environments*, 51(2), 235-254.

[49] Wang, Z.H., Bou-Zeid, E., and Smith, J.A. (2011). A spatially-analytical scheme for surface temperatures and conductive heat fluxes in urban canopy models. *Boundary-Layer Meteorology*, 138(2), 171-193.

[50] Wang, Z.H., Bou-Zeid, E., and Smith, J.A. (2013). A coupled energy transport and hydrological model for urban canopies evaluated using a wireless sensor network. *Quarterly Journal of the Royal Meteorological Society*, 139(675), 1643-1657.

[51] Yang, J., Wang, Z.H., Chen, F., Miao, S., Tewari, M., Voogt, J., et al. (2015b). Enhancing hydrologic modeling in the coupled Weather Research and Forecasting - urban modeling system. *Boundary-Layer Meteorology*, 155(1), 87-109.

[52] Ryu, Y.H., Bou-Zeid, E., Wang, Z.H., and Smith, J.A. (2016). Realistic representation of urban trees in an urban canopy model. *Boundary-Layer Meteorology*, 159, 193-220.

[53] Li, P., and Wang, Z.H. (2020), Modeling carbon dioxide exchange in a single-layer urban canopy model, *Building and Environment*, 184, 107243.

[54] Wang, C., Wang, Z.H., and Ryu, Y.H. (2021b). A single-layer urban canopy model with transmissive radiation exchange between trees and street canyons. *Building and Environment*, 191, 107593.

[55] Song, J., and Wang, Z.H. (2015b). Interfacing the urban land–atmosphere system through coupled urban canopy and atmospheric models. *Boundary-layer meteorology*, 154, 427-448.

[56] Yang, J., Wang, Z.H., Georgescu, M., Chen, F., and Tewari, M. (2016), Assessing the impact of enhanced hydrological processes on urban hydrometeorology with application to two cities in contrasting climates, *Journal of Hydrometeorology*, 17, 1031-1047.

[57] Lipson, M.J., Grimmond, S., Best, M., Abramowitz, G., Coutts, A., Tapper, N., et al. (2024), Evaluation of 30 urban land surface models in the Urban-PLUMBER project: Phase 1 results, *Quarterly Journal of the Royal Meteorological Society*, 150(758), 126-169.

[58] Brutsaert, W. (2005). *Hydrology–An Introduction*, Cambridge University Press, Cambridge, 605.

[59] Sun, T., Bou-Zeid, E., and Ni, G.H. (2014). To irrigate or not to irrigate: Analysis of green roof performance via a vertically-resolved hygrothermal model. *Building and Environment*, 73, 127-137.

[60] Wang, C., Wang, Z.H., and Li, Q. (2020), Emergence of urban clustering among U.S. cities under environmental stressors, *Sustainable Cities and Society*, 63, 102481.

[61] Yang, X., Wang, Z.H., Wang, C., and Lai, Y.C. (2022), Detecting the causal influence of thermal environments among climate regions in the United States, *Journal of Environmental Management*, 322, 116001.

[62] Yang, X., Wang, Z.H., Wang, C., and Lai, Y.C. (2024), Megacities are causal pacemakers of extreme heatwaves, *npj Urban Sustainability*, 4, 8.